



# Remarks on the asymptotic behaviour of Koiter shells

F. Auricchio<sup>a</sup>, L. Beirão da Veiga<sup>b</sup>, C. Lovadina<sup>b,\*</sup>

<sup>a</sup> *Dipartimento di Meccanica Strutturale, Università di Pavia, Via Ferrata 1, I-27100 Pavia, Italy*

<sup>b</sup> *Dipartimento di Matematica, Università di Pavia, Via Ferrata 1, I-27100 Pavia, Italy*

Accepted 1 February 2002

## Abstract

We review some results about the behaviour of a general Koiter shell, in the framework of linear elasticity. In particular, we investigate the asymptotics (for the thickness tending to zero) of the energy functional and of the percentage of the energy which is stored in the bending term. Such an analysis is motivated by the need to better understand how to numerically treat an arbitrary thin shell, when the discretization is performed using a finite element strategy. We present some instances to which our theory can be applied. Some numerical tests confirming our theoretical predictions are also provided. © 2002 Elsevier Science Ltd. All rights reserved.

*Keywords:* Koiter shells; Energy estimates; Real interpolation theory; Finite element method

## 1. Introduction

Although thin shell structures are widely encountered in engineering practice, it is commonly accepted that their analysis still needs much more investigations. One of the main difficulties stands in the large variety of *different* structural responses of a general shell, depending on its geometric shape, on the applied loads and on the boundary conditions. A reliable shell finite element must capture all the possible behaviours of the structure. The procedure of finding a finite element solution can be summarized by the following steps (cf. [1]).

- (1) Choice of the shell physical problem.
- (2) Choice of a mathematical model to describe the physical problem: Koiter's (based on Kirchhoff–Love assumptions), Naghdi's (based on Reissner–Mindlin assumptions) or other models. For this topic we refer for example to [2–5].
- (3) Choice of a finite element discretization for the selected mathematical model.

In this note, we will only deal with the Koiter's model (see, for instance, [4,6]), but similar considerations can be developed for other models as well. It should be noted that finding a strategy to successfully discretize the problem by means of a finite element scheme is not at all a trivial task, because the shell “asymptotic stiffness” (as the thickness tends to zero), may vary depending on the shell geometry, the loads and the boundary conditions. For example, when the stiffness of the structure is of order  $\varepsilon^3$  as  $\varepsilon \rightarrow 0$  ( $\varepsilon$  being the shell thickness), most of the elastic energy is typically stored in the *bending* part; in this case a modification of the membrane energy term is needed at the discrete level, in order to avoid locking effects (cf. for instance [1,7]). On the contrary, when the stiffness is of order  $\varepsilon$  as  $\varepsilon \rightarrow 0$ , most of the energy is carried by the *membrane* term; for such a situation a modification of the membrane energy may cause undesirable numerical instabilities. To continue, there are cases in which neither the bending energy nor the membrane one *asymptotically* dominates (see [8]). We will refer to them as *intermediate shells*. They often arise when the shell geometry, the loads and the boundary conditions cause boundary or interior layers where a significant part of the energy is concentrated. Due to this complexity, the theoretical analysis of convergence and stability for finite elements to be used *for a general shell*

\* Corresponding author.

E-mail address: [lovadina@dimat.unipv.it](mailto:lovadina@dimat.unipv.it) (C. Lovadina).

problem is still missing. Therefore, it is of fundamental importance to test a finite element scheme on a suitable set of benchmarks, as highlighted in [1]. Such numerical tests have been used, for example, to investigate the features of shell elements based on the MITC approach (see [9]), showing that these schemes provide effective discretization procedures. We also notice that the “limit process” mentioned above, which is obviously never implemented in actual computations, mimic somehow the *real* situation when the thickness is small compared to the other characteristic dimensions of the shell. It turns out that the analysis of finite elements for thin shells require a good knowledge on the asymptotic behaviour of the structure stiffness, and therefore on its elastic energy, as pointed out in [10].

The purpose of this paper is to report some of our results concerning the asymptotic of an arbitrary shell problem, focusing our attention on the energy functional and on the percentage of energy which is stored in the bending term. We point out that we are not going to detail any proof of theorems and propositions, for which we mainly refer to [11–13].

The paper is organized as follows. In Section 2 we briefly introduce the Koiter shell problem together with the necessary notations and definitions. In particular, we define the concept of *problem order*, whose meaning is roughly the following: we say that a shell problem is of order  $\alpha$  if its elastic energy is proportional to  $\varepsilon^{-\alpha}$  for  $\varepsilon \rightarrow 0$ . In Section 3 we review the basic energy estimates. In treating the intermediate shells, our main tool is the real interpolation theory, for which we refer to [14,15]. We wish to remark that interpolation theory was already employed in [16] to study a singularly perturbed problem. Section 4 is dedicated to a result concerning the connection between the problem order and the percentage of bending energy. Finally, Section 5 provides several examples of application of our theory, together with some numerical tests. With this respect, we wish to stress that much more detailed and exhaustive numerical investigations have been recently presented in [17].

## 2. The Koiter shell problem

Let  $(e_1, e_2, e_3)$  be the usual orthonormal basis for the Euclidean space  $\mathbf{R}^3$  equipped with the standard inner product. We denote by  $u \cdot v$  the inner product between two vectors in  $\mathbf{R}^3$ , by  $|u| = \sqrt{u \cdot u}$  the associated norm and by  $u \wedge v$  the exterior product between them. In the sequel, greek subscripts will take their values in the set  $\{1, 2\}$  while latin subscripts will take their values in the set  $\{1, 2, 3\}$ . We will also employ the Einstein summation convention. Let  $\omega$  be a regular domain in  $\mathbf{R}^2$ . We consider a shell with midsurface  $S = \varphi(\bar{\omega})$ , where  $\varphi$  is a sufficiently regular injective map such that the vectors  $a_\alpha = \partial_\alpha \varphi$  are linearly independent at each point of  $\bar{\omega}$ . We

define the unit normal vector to the surface at point  $\varphi(x)$  as  $a_3 = a_1 \wedge a_2 / |a_1 \wedge a_2|$ . We recall that the vectors  $a_i(x)$  define the covariant basis at  $\varphi(x)$ . The contravariant basis  $a^j$  is defined by the relations  $a_i \cdot a^j = \delta_i^j$  (note that  $a^3 = a_3$ ). We furthermore set  $a(x) = |a_1(x) \wedge a_2(x)|^2$ . The Christoffel symbols of the surface are given by  $\Gamma_{\alpha\beta}^\rho = \Gamma_{\beta\alpha}^\rho = a^\rho \cdot \partial_\beta a_\alpha$ . Let us introduce the following Hilbert space (cf. [18]):

$$\mathcal{U} = \{v \in H^1(\omega; \mathbf{R}^3) : \partial_{\alpha\beta} v \cdot a_3 \in L^2(\omega)\} \cap \mathcal{BC} \tag{1}$$

equipped with the norm

$$\|v\|_{\mathcal{U}} = (\|v\|_{H^1(\omega; \mathbf{R}^3)}^2 + \sum_{\alpha, \beta} \|\partial_{\alpha\beta} v \cdot a_3\|_{L^2(\omega)}^2)^{1/2}. \tag{2}$$

Above,  $\mathcal{BC}$  symbolically means that the appropriate kinematic boundary conditions are enforced in the space  $\mathcal{U}$ . It is well known that the Koiter problem for a shell of thickness  $\varepsilon$  (cf. [14,18]) can be written in a variational formulation as

$$\begin{cases} \text{find } u_\varepsilon \in \mathcal{U} \text{ such that,} \\ \varepsilon a^m(u_\varepsilon, v) + \varepsilon^3 a^b(u_\varepsilon, v) = \langle f, v \rangle \quad \forall v \in \mathcal{U}, \end{cases} \tag{3}$$

where

$$a^m(u, v) = \int_\omega a^{\alpha\beta\rho\sigma} \gamma_{\alpha\beta}(u) \gamma_{\rho\sigma}(v) \sqrt{a} \, dx \tag{4}$$

and

$$a^b(u, v) = \frac{1}{12} \int_\omega a^{\alpha\beta\rho\sigma} \Upsilon_{\alpha\beta}(u) \Upsilon_{\rho\sigma}(v) \sqrt{a} \, dx. \tag{5}$$

In (4) and (5),  $a^{\alpha\beta\rho\sigma}$  is an elasticity tensor satisfying the usual symmetry and positive-definiteness conditions,

$$\gamma_{\alpha\beta}(u) = \frac{1}{2}(\partial_\alpha u \cdot a_\beta + \partial_\beta u \cdot a_\alpha) \in L^2(\omega) \tag{6}$$

is the deformation tensor, while

$$\Upsilon_{\alpha\beta}(u) = (\partial_{\alpha\beta} u - \Gamma_{\alpha\beta}^\rho \partial_\rho u) \cdot a_3 \in L^2(\omega) \tag{7}$$

is the tensor of linearized change of curvature of the shell midsurface, both given by their covariant components. Note that  $a^m(\cdot, \cdot)$  is related to the elastic membrane energy, while  $a^b(\cdot, \cdot)$  to the elastic bending energy. Moreover,  $\mathcal{U}$  is the space of admissible displacements (the ones having finite elastic energy), which also takes into account the kinematical boundary conditions (see (1)). Finally,  $f$  belongs to  $\mathcal{U}'$ , the topological dual space of  $\mathcal{U}$ , and represents the loads applied to the structure. We remark (cf. [4]) that both  $a^m(\cdot, \cdot)$  and  $a^b(\cdot, \cdot)$  are symmetric  $\mathcal{U}$ -continuous forms, and the sum  $a^m(\cdot, \cdot) + a^b(\cdot, \cdot)$  is coercive on  $\mathcal{U}$ . It follows from the Lax–Milgram lemma that for each  $\varepsilon > 0$  the Koiter problem (3) has a unique solution  $u_\varepsilon \in \mathcal{U}$  (see [4,18,19]). We also recall (see [20]) that

$$\mathcal{U}_1 = \{v \in \mathcal{U}, a^m(v, w) = 0, \quad \forall w \in \mathcal{U}\} \tag{8}$$

is the inextensional (or pure bending) displacement space of the midsurface. Thanks to the continuity of the form  $a^m(\cdot, \cdot)$  on  $\mathcal{U}$ ,  $\mathcal{U}_1$  is a closed subspace of  $\mathcal{U}$ . Let us denote by  $\mathcal{U}_1^0 \subset \mathcal{U}'$  the polar set of  $\mathcal{U}_1$ , i.e.

$$\mathcal{U}_1^0 = \{f \in \mathcal{U}' \mid \langle f, v \rangle = 0, \quad \forall v \in \mathcal{U}_1\}. \tag{9}$$

From a mechanical point of view, the elements of  $\mathcal{U}_1^0$  are those loads which do not activate any inextensional displacement. Notice also that when  $\mathcal{U}_1 = (0)$ , then  $\mathcal{U}_1^0$  is the whole space  $\mathcal{U}'$ . The orthogonal space of  $\mathcal{U}_1$  in  $\mathcal{U}$  is given by

$$V := \{u \in \mathcal{U}, a^b(u, v) = 0, \quad \forall v \in \mathcal{U}_1\}, \tag{10}$$

when  $\mathcal{U}$  is equipped with the inner product  $(a^m(u, v) + a^b(u, v))$ . Clearly,  $V$  is a Hilbert space, with the norm inherited by  $\mathcal{U}$ . Thus, we have

$$\mathcal{U} = \mathcal{U}_1 \oplus V. \tag{11}$$

In the sequel, we will see that the following space:

$W$  = the completion of  $V$  with the norm

$$a^m(v, v)^{1/2} := \|v\|_W, \tag{12}$$

will play a crucial role. Note that on  $V$   $\|v\|_W$  is indeed a norm, not only a seminorm. We also remark that typically  $\|\cdot\|_W$  is weaker than  $\|\cdot\|_V$ , since  $W$  can be viewed as the space of (generalized) displacements for which we require that *only* the membrane energy is finite. We now introduce the *energy functional* defined by

$$E(\varepsilon, v) := \varepsilon a^m(v, v) + \varepsilon^3 a^b(v, v) \quad \forall v \in \mathcal{U}. \tag{13}$$

The aim of this Note is to report some of our results on the asymptotic behaviour (as  $\varepsilon \rightarrow 0$ ) of the energy functional, when tested on the solution  $u_\varepsilon \in \mathcal{U}$  of problem (3). We then set

$$E(\varepsilon) := E(\varepsilon, u_\varepsilon) = \varepsilon a^m(u_\varepsilon, u_\varepsilon) + \varepsilon^3 a^b(u_\varepsilon, u_\varepsilon). \tag{14}$$

Hence (cf. (3))

$$E(\varepsilon) = \langle f, u_\varepsilon \rangle. \tag{15}$$

It should be clear that, independently of  $f \in \mathcal{U}'$  different from zero, the function  $E(\varepsilon)$  in (14) goes to infinity as  $\varepsilon \rightarrow 0$  (for a proof see [21]). Our idea consists in classifying the asymptotic shell behaviours by analyzing the rate of blowing up of the energy  $E(\varepsilon)$  (see [11]). More precisely, we introduce the following.

**Definition 1.** Given  $f \in \mathcal{U}'$ , we say that the Koiter problem (3) is of order  $\alpha$  if

$$\alpha = \inf \{ \beta \mid \varepsilon^\beta E(\varepsilon) \in L^\infty(0, 1) \}. \tag{16}$$

The meaning of the above definition is that the problem is of order  $\alpha$  when the energy  $E(\varepsilon)$  essentially behaves like  $\varepsilon^{-\alpha}$ . It is not hard to show that (cf. [21,22]) if the

Koiter problem (3) is of order  $\alpha$  then  $1 \leq \alpha \leq 3$ . We will see in the next sections that the problem order is strictly linked to the “regularity” of the datum  $f \in \mathcal{U}'$ . We conclude this section by noting that if  $f \in \mathcal{U}_1^0$  (cf. (9)), then the Koiter problem (3) can be equivalently formulated as (see [1])

$$\begin{cases} \text{find } u_\varepsilon \in V \text{ such that,} \\ \varepsilon a^m(u_\varepsilon, v) + \varepsilon^3 a^b(u_\varepsilon, v) = \langle f, v \rangle \quad \forall v \in V, \end{cases} \tag{17}$$

where  $V$  is defined by (10). As a consequence, in the sequel we will refer to problem (3) if  $f \notin \mathcal{U}_1^0$ , and to problem (17) if  $f \in \mathcal{U}_1^0$ .

### 3. Energy estimates and problem orders

In this section we will review some energy estimates for a general shell, by distinguishing among the following three fundamental different situations concerning the datum  $f$ .

#### 3.1. Bending dominated shell: the case $f \notin \mathcal{U}_1^0$

This case occurs when  $\mathcal{U}_1 \neq (0)$  and there are pure bending displacements which are activated by the loads  $f$  imposed to the structure. It turns out that the stiffness of the shell behaves like  $\varepsilon^3$  and the energy like  $\varepsilon^{-3}$ . In fact, it is well known that the following result holds true (cf. [23,24], for instance).

**Theorem 2.** Fix  $f \notin \mathcal{U}_1^0$  and consider the problem

$$\begin{cases} \text{find } u_\varepsilon \in \mathcal{U} \text{ such that,} \\ \varepsilon a^m(u_\varepsilon, v) + \varepsilon^3 a^b(u_\varepsilon, v) = \langle f, v \rangle \quad \forall v \in \mathcal{U}. \end{cases} \tag{18}$$

Then problem (18) is of order  $\alpha = 3$ . Furthermore, let  $u_b \in \mathcal{U}_1$  be the solution of the bending-type problem

$$\begin{cases} \text{find } u_b \in \mathcal{U}_1 \text{ such that,} \\ a^b(u_b, v_0) = \langle f, v_0 \rangle \quad \forall v_0 \in \mathcal{U}_1. \end{cases} \tag{19}$$

Then, as  $\varepsilon \rightarrow 0$ ,

$$\| \varepsilon^3 u_\varepsilon - u_b \|_{\mathcal{U}} \rightarrow 0, \quad E(\varepsilon) \approx \varepsilon^{-3}, \quad \frac{\varepsilon^3 a^b(u_\varepsilon, u_\varepsilon)}{E(\varepsilon)} \rightarrow 1. \tag{20}$$

Moreover,  $u_b \neq 0$ .

We notice that in this case the *scaled solution*  $\varepsilon^3 u_\varepsilon$  converges to a well-defined limit  $u_b$ , which is indeed a non-trivial inextensional displacement. Furthermore, the whole elastic energy is asymptotically stored in the bending part. We end this subsection by a remark about the stability of this case with respect to load perturbations. Since  $\mathcal{U}_1^0$  is a closed subspace of  $\mathcal{U}'$  (being the polar set of the subspace  $\mathcal{U}_1$ ), its complement

$$\mathcal{C}\mathcal{W}_1^0 = \{g \in \mathcal{W}' : g \notin \mathcal{W}_1^0\} \tag{21}$$

is an open set of  $\mathcal{W}'$ . It follows that if  $f \notin \mathcal{W}_1^0$  (i.e.  $f \in \mathcal{C}\mathcal{W}_1^0$ ), then there is an open ball  $B(f, r)$  of  $\mathcal{W}'$ , centered in  $f$  and of radius  $r > 0$ , which is *entirely* contained in  $\mathcal{C}\mathcal{W}_1^0$ . This means that for every load  $\delta f$  such that  $\|\delta f\|_{\mathcal{W}'} < r$ , the perturbed load  $f + \delta f$  still belongs to  $\mathcal{C}\mathcal{W}_1^0$ . As a consequence, small perturbations of the load do not change the type of asymptotic behaviour of the shell.

3.2. Membrane dominated shell: the case  $f \in \mathcal{W}_1^0$  and  $f \in W'$

As already noticed, for this case we refer to problem (17). Moreover, from (12) the assumption  $f \in W'$ , the topological dual space of  $W$ , is equivalent to the existence of a constant  $C$  such that

$$\langle f, v \rangle \leq C a^m(v, v)^{1/2} \quad \forall v \in V. \tag{22}$$

Hence,  $f \in W'$  means that the shell is able to control the external work *only by means of the membrane energy for every admissible displacement*. This is typically a very strong requirement and fails to be satisfied in many instances, as we will see in the next section. We also remark that in some cases the space  $W'$  is so “small” that it does not contain the space of compactly supported regular functions (cf. [25]). However, if  $f \in \mathcal{W}_1^0$  and  $f \in W'$  we have the following (cf. [20]).

**Theorem 3.** Fix  $f \in \mathcal{W}_1^0$  and suppose moreover that  $f \in W'$ , where  $W'$  is the dual space of  $W$  (cf. (12)). Consider the problem

$$\begin{cases} \text{find } u_\varepsilon \in V \text{ such that,} \\ \varepsilon a^m(u_\varepsilon, v) + \varepsilon^3 a^b(u_\varepsilon, v) = \langle f, v \rangle \quad \forall v \in V. \end{cases} \tag{23}$$

Then problem (23) is of order  $\alpha = 1$ . Furthermore, let  $u_m \in W$  be the solution of the membrane-type problem

$$\begin{cases} \text{find } u_m \in W \text{ such that,} \\ a^m(u_m, v_0) = \langle f, v_0 \rangle \quad \forall v_0 \in W. \end{cases} \tag{24}$$

Then

$$\|\varepsilon u_\varepsilon - u_m\|_W \rightarrow 0, \quad E(\varepsilon) \approx \varepsilon^{-1}, \quad \frac{\varepsilon^3 a^b(u_\varepsilon, u_\varepsilon)}{E(\varepsilon)} \rightarrow 0 \tag{25}$$

as  $\varepsilon \rightarrow 0$ . Moreover,  $u_m \neq 0$ .

We notice that in this case the *scaled solution*  $\varepsilon u_\varepsilon$  converges to a well-defined limit  $u_m$ , at least in the weak space  $W$ . Moreover, the stiffness of the shell behaves like  $\varepsilon$  and the energy like  $\varepsilon^{-1}$ . Finally, the whole elastic energy is asymptotically stored in the membrane part.

3.3. Intermediate shells: the case  $f \in \mathcal{W}_1^0$  but  $f \notin W'$

These are surely the most subtle cases to deal with. From a mechanical point of view, they typically arise when either the irregularity of  $f$  or the assumed boundary conditions, together with the geometric shape of the shell, cause boundary or interior layers which carry a significant part of the elastic energy. Again, we will refer to problem (17), since  $f \in \mathcal{W}_1^0$ . But now  $f \notin W'$ , so that (22) is not satisfied. Since, by duality,  $W'$  is densely contained in  $V'$  and  $f \in V'$ , it follows that  $f$  should be “somewhere in-between”  $W'$  and  $V'$ . Thus, it is reasonable to use the real interpolation theory (see e.g. [14,15] for the details), which gives us a scale of spaces  $(W', V')_{\theta, 2}$  ( $0 < \theta < 1$ ) between  $W'$  and  $V'$ . We found that the behaviour of the elastic energy (and so the problem order) is strictly related to “the smallest” interpolated space which  $f$  belongs to (see [11]). More precisely, we have the following theorem (cf. Definition 1).

**Theorem 4.** Fix  $f \in V'$  and consider the problem

$$\begin{cases} \text{find } u_\varepsilon \in V \text{ such that,} \\ \varepsilon a^m(u_\varepsilon, v) + \varepsilon^3 a^b(u_\varepsilon, v) = \langle f, v \rangle \quad \forall v \in V. \end{cases} \tag{26}$$

(1) If  $f \in (W', V')_{\theta, 2}$  for some  $0 < \theta < 1$ , then problem (26) is of order  $\alpha$  given by

$$\alpha = \inf\{2\theta + 1 : f \in (W', V')_{\theta, 2}, \quad 0 < \theta < 1\}. \tag{27}$$

(2) If  $f \notin (W', V')_{\theta, 2}$  for any  $0 < \theta < 1$ , then problem (26) is of order  $\alpha = 3$ .

A consequence of the above theorem is

**Corollary 5.** If problem (26) is of order  $\alpha$ , then it holds the following.

- (1) If  $\beta > \alpha$  then  $\lim_{\varepsilon \rightarrow 0} (\varepsilon^\beta E(\varepsilon)) = 0$ .
- (2) If  $1 \leq \beta < \alpha$  then  $\limsup_{\varepsilon \rightarrow 0} (\varepsilon^\beta E(\varepsilon)) = +\infty$ .
- (3) If  $\beta < 1$  then  $\lim_{\varepsilon \rightarrow 0} (\varepsilon^\beta E(\varepsilon)) = +\infty$ .

We notice that in these intermediate cases we do not have  $E(\varepsilon) \approx \varepsilon^{-\alpha}$ ; however, Corollary 5 says that  $\alpha$  is the best exponent to “nearly” have  $E(\varepsilon) \approx \varepsilon^{-\alpha}$ . Moreover, we are not able, in general, to prove that the *scaled solution*  $\varepsilon^\alpha u_\varepsilon$  converges in a suitable norm to any  $u_x$ , solution of a limit problem. Results in this direction would be of great interest, since they would likely provide some useful hint on the strategies to apply for the numerical treatment of such situations.

We conclude this section with a brief discussion about the effect of a load perturbation on a shell problem for which  $f \in \mathcal{W}_1^0$  (i.e. the cases described in Sections 3.2 and 3.3). In what follows we will consider only perturbations  $\delta f$  which are compactly supported regular functions. We distinguish two different situations.

(1) The subspace of pure bending displacements is not trivial (i.e.  $\mathcal{U}_1 \neq (0)$ ). In this case  $\mathcal{U}_1^0$  is a closed subspace strictly contained in  $\mathcal{U}$ . It follows that there are arbitrarily small perturbations  $\delta f$  such that  $(f + \delta f) \notin \mathcal{U}_1^0$ , even though  $f \in \mathcal{U}_1^0$ . As a consequence, the perturbed shell problem may fall into the category of Section 3.1, thus changing its asymptotic behaviour. We remark that this kind of instability can be very strong: if we consider an initial load  $f \in W'$ , the shell energy is of order  $\varepsilon^{-1}$  (cf. Section 3.2), while for  $(f + \delta f) \notin \mathcal{U}_1^0$  the shell energy is of order  $\varepsilon^{-3}$  (cf. Section 3.1). For more details on such a loss of stability, we refer to [1,3].

(2) The subspace of pure bending displacements is trivial (i.e.  $\mathcal{U}_1 = (0)$ ). It follows that  $\mathcal{U} = V$  and  $\mathcal{U}_1^0 = V'$ . For this case, the effect of “small and regular” perturbations  $\delta f$  depends on the structure of the space  $W'$ . More precisely, if  $W'$  does not contain the space of compactly supported regular functions (i.e. the shell is sensitive, cf. [25]), a small perturbation  $\delta f$  may change the asymptotic behaviour of the shell problem. This is easily seen, for example, by considering  $f \in W'$  (hence we are in the framework of Section 3.2). The new load  $f + \delta f$  belongs to  $V'$  but it may happen that it is not in  $W'$  anymore, so that the perturbed problem will fall into the category of Section 3.3. On the contrary, if  $W'$  contains the space of “regular” functions, the perturbation  $\delta f$  does not change the asymptotic behaviour of the shell.

Of course, the above considerations are neither rigorous nor exhaustive, and should be intended only to remark once again how complex the general shell problem is. A satisfactory investigation would require, for instance, to identify the relevant norms to be used for the stability analysis.

#### 4. The ratio bending/total energy

In this short section we will consider the asymptotic ratio between the bending energy and the total elastic energy (bending energy percentage), i.e. we will focus on the function  $R(\varepsilon)$ , defined as

$$R(\varepsilon) := \frac{\varepsilon^3 a^b u_\varepsilon, u_\varepsilon}{E(\varepsilon)}. \tag{28}$$

We were able to prove the following theorem (see [11]).

**Theorem 6.** Consider a shell problem of order  $\alpha$ . Moreover, suppose that there exist

$$+\infty > \lim_{\varepsilon \rightarrow 0} (\varepsilon^\alpha E(\varepsilon)) > 0, \quad \lim_{\varepsilon \rightarrow 0} \varepsilon^{\alpha+3} a^b(u_\varepsilon, u_\varepsilon) \geq 0. \tag{29}$$

Then it holds

$$\lim_{\varepsilon \rightarrow 0} R(\varepsilon) = \frac{\alpha - 1}{2}. \tag{30}$$

**Remark 7.** By analysing the work [22], Sanchez-Palencia conjectured that a relationship between  $\alpha$  and  $R(\varepsilon)$  might hold. Our Theorem 6 answers in a positive way this question.

**Remark 8.** We also remark that, in general, we are not able to prove that (29) hold. However, as we have already seen, in the hypotheses of Theorem 2 (resp.: Theorem 3),  $\alpha = 3$  (resp.:  $\alpha = 1$ ) and (29) are satisfied. For intermediate shells, Eq. (30) says that neither the bending nor the membrane energy asymptotically dominates upon the other one.

### 5. Applications and numerical tests

The aim of this section is to present some instances of shell problems, focusing our attention on the behaviour of both the total elastic energy and the bending energy percentage. For some of the following problems we can rigorously apply our theory to predict the asymptotic response of the shell. In other cases, due to the complexity of the membrane form, we were able to use our theorems, developing only a “partial” analysis based on heuristic considerations, which led us to formulate some conjectures about the shell behaviour. Numerical tests supporting our results are also presented below.

#### 5.1. The “Pitkäranta’s cylinder”

The aim of this subsection is to report our analysis about a shell of intermediate order, inspired by the considerations of [8]. We consider a cylindrical shell of thickness  $\varepsilon$ , described by the region

$$\Omega = \{(x, \varphi, z) \mid -1 \leq x \leq 1, \quad 0 \leq \varphi \leq 2\pi, \\ -\varepsilon/2 \leq z \leq \varepsilon/2\}. \tag{31}$$

Above,  $x$  is the axial coordinate,  $\varphi$  the angular one and  $z$  the radial one. We call  $\omega$  the midsurface of the shell. We will suppose that the shell is acted upon an axially constant normal pressure distribution which varies angularly as

$$f = f_0 \cos \varphi, \tag{32}$$

where  $f_0$  is a constant. As far as the boundary conditions are concerned, we suppose that the normal displacements are set to zero at both ends of the cylinder, while the other displacement components are free. Due to the particular shape of the load and boundary conditions, the problem can be reduced to a one-dimensional (1D) (axially) problem (cf. [8]), whose unknown are  $u = u(x)$  (the axial displacement),  $v = v(x)$  (the angular displacement) and  $w = w(x)$  (the radial or normal displacement).

Furthermore, the membrane strains are given by

$$\gamma_{11} = u', \quad \gamma_{12} = \frac{1}{2}(-u + v'), \quad \gamma_{22} = v + w, \tag{33}$$

while the bending strains are

$$\Upsilon_{11} = w'', \quad \Upsilon_{12} = \frac{1}{2}(-v' - w'), \quad \Upsilon_{22} = -v - w. \quad (34)$$

Introducing the notation  $\underline{u} = (u, v, w)$ , the membrane and bending energy forms are given by

$$\begin{aligned} \varepsilon a^m(\underline{u}, \underline{u}) := & \frac{\varepsilon}{2} \int_{-1}^1 \left[ v(\gamma_{11}(\underline{u}) + \gamma_{22}(\underline{u}))^2 \right. \\ & \left. + (1 - \nu) \sum_{i,j=1}^2 \gamma_{ij}(\underline{u}) \right] dx, \end{aligned} \quad (35)$$

$$\begin{aligned} \varepsilon^3 a^b(\underline{u}, \underline{u}) := & \frac{\varepsilon^3}{24} \int_{-1}^1 \left[ v(\Upsilon_{11}(\underline{u}) + \Upsilon_{22}(\underline{u}))^2 \right. \\ & \left. + (1 - \nu) \sum_{i,j=1}^2 \Upsilon_{ij}(\underline{u}) \right] dx, \end{aligned}$$

where  $\nu$  is the Poisson's ratio. Next, the external energy is given by

$$\langle f, \underline{u} \rangle = \int_{-1}^1 f_0 w dx. \quad (36)$$

For this shell, the admissible displacement space is given by

$$\mathcal{U} = H^1(-1, 1) \times H^1(-1, 1) \times (H^2(-1, 1) \cap H_0^1(-1, 1)) \quad (37)$$

with the usual norm. Moreover, it is easily seen that (cf. (8))

$$\mathcal{U}_1 = \{ \underline{u} \in \mathcal{U}, a^m(\underline{u}, \underline{u}) = 0, \quad \forall \underline{u} \in \mathcal{U} \} = 0. \quad (38)$$

Hence,  $\mathcal{U} = V$  (cf. (10) and (11)) and  $f \in \mathcal{U}_1^0 = V'$ . For this shell we were able to *rigorously prove* (cf. [11]) that the problem order is  $\alpha = 3/2$ . We remark that this result is in perfect agreement with the numerical tests detailed in [8].

### 5.2. Other cylindrical shell problems

We now consider a cylindrical shell with thickness  $\varepsilon$ . The length of the cylinder is now set to 5, while the boundary conditions correspond to clamp the displacements in the normal direction at both ends of the shell. We will consider two problems by choosing the following two different loads: the first load  $f_1$  is a Dirac ring of “squeezing” force, while the load  $f_2$  is a Dirac ring of moments. Both loads will lead to intermediate shells, as we will see in what follows. Due to the rotational symmetry of the boundary conditions and applied loads, we can easily obtain in both cases a 1D (axially) formulation, whose unknown is  $\underline{u} = (u_1, u_2)$ , where  $u_1 = u_1(x)$  is the axial displacement and  $u_2 = u_2(x)$  is the normal displacement. For these shell problems we have

- (1) the bending and membrane bilinear forms are

$$\begin{aligned} a^b(\underline{u}, \underline{v}) = & \frac{E}{12(1 - \nu^2)} \int_0^5 [(u_2'' v_2'' + u_2 v_2) \\ & + \nu(-u_2'' v_2 - u_2 v_2')] dx, \end{aligned} \quad (39)$$

$$\begin{aligned} a^m(\underline{u}, \underline{v}) = & \frac{E}{1 - \nu^2} \int_0^5 [(u_1' v_1' + u_2 v_2) \\ & + \nu(u_1' v_2 + u_2 v_1')] dx, \end{aligned} \quad (40)$$

where  $E$  is the Young's modulus and  $\nu$  is the Poisson's ratio,

(2) the loads are

$$\langle f_1, \underline{v} \rangle = -Kv_2(\frac{5}{2}), \quad \langle f_2, \underline{v} \rangle = -Kv_2'(\frac{5}{2}), \quad (41)$$

where  $K$  is a positive constant

(3) the space  $\mathcal{U}$  is given by

$$\mathcal{U} = (H^1(0, 5)/\mathcal{R}) \times H_0^2(0, 5),$$

where the quotient by the rigid body displacements  $\mathcal{R}$  is introduced only to have a unique solution.

It is straightforward to check that  $\mathcal{U} = V$  (cf. (10) and (11)) and  $f_i \in \mathcal{U}_1^0 = V'$ . Therefore, due to (40) and by basic interpolation theory, we easily obtain

$$W = (H^1(0, 5)/\mathcal{R}) \times L^2(0, 5), \quad (42)$$

$$(W', V')_{0,2} = (H^1(0, 5)/\mathcal{R})' \times (H^{2,0}(0, 5))'. \quad (43)$$

Consequently, considering (43) and the Sobolev regularity of the loads, it follows

$$f_1 \in (W', V')_{0,2} \iff \theta > \frac{1}{4}, \quad f_2 \in (W', V')_{0,2} \iff \theta > \frac{3}{4}, \quad (44)$$

which, applying Theorem 4, implies

$$\begin{aligned} \alpha_1 = & \inf \{ 2\theta + 1 : \theta > \frac{1}{4} \} = \frac{3}{2}, \\ \alpha_2 = & \inf \{ 2\theta + 1 : \theta > \frac{3}{4} \} = \frac{5}{2}, \end{aligned} \quad (45)$$

where  $\alpha_1$  and  $\alpha_2$  are the problem orders corresponding to  $f_1$  and  $f_2$ .

As a *numerical test* we computed accurate approximated solutions  $\underline{u}_h$  by means of a classical finite element scheme. More precisely, we employed piecewise linear  $\mathcal{C}^0$  functions for the first component of the displacements, and piecewise cubic  $\mathcal{C}^1$  functions for the second one. In order to get a very accurate discrete solution we used a mesh particularly refined around the load application point. Thus, we have no doubts about the reliability of our computations. For both problems we calculated the corresponding total elastic energy

$$E_h(\varepsilon) = \varepsilon a^m(\underline{u}_h, \underline{u}_h) + \varepsilon^3 a^b(\underline{u}_h, \underline{u}_h) \quad (46)$$

for different values of the thickness. We found that the energy strictly follows thickness dependence laws of the type

$$E_h(\varepsilon) \approx \varepsilon^{-3/2} \quad \text{for load } f_1, \tag{47}$$

$$E_h(\varepsilon) \approx \varepsilon^{-5/2} \quad \text{for load } f_2, \tag{48}$$

which imply a problem order of 3/2 for load  $f_1$  and 5/2 for load  $f_2$ . These energy behaviours can be appreciated in Fig. 1, plotting the logarithm of  $E_h(\varepsilon)$  vs the logarithm of  $\varepsilon$ . The rectilinear shape of the graphs, respectively with slopes  $-3/2$  and  $-5/2$ , clearly highlights an energy thickness dependence of type (47) and (48). Therefore the numerical results completely confirm the behaviour predicted by the theory (see (45)). Also, we computed the ratio between the bending energy and the total energy

$$R_h(\varepsilon) = \frac{\varepsilon^3 a^b(\underline{u}_h, \underline{u}_h)}{E_h(\varepsilon)}, \tag{49}$$

obtaining a very quick convergence, as  $\varepsilon \rightarrow 0$ , to the values predicted by Theorem 6 (respectively, 1/4 and 3/4).

We conclude this subsection by remarking that we have also obtained some rigorous error estimates (which are uniform in the thickness) for the finite element discretization of the cylindrical shell subjected to load  $f_1$  (see [13]). Even though our analysis covers only the case of a  $P3$ – $P5$  conforming element, we nonetheless believe that our technique can be extended to other schemes.

### 5.3. Toroidal shell problems

We analyze three different problems for a toroidal shell of thickness  $\varepsilon$ . In all three cases, a ring-shaped load in the normal direction is acting on the torus; what changes in each problem is the position of the ring. Similarly to the cylindrical case, the rotational symmetry leads to a 1D problem on the torus circular section, whose unknown is  $\underline{u} = (u_1, u_2)$ , where  $u_1 = u_1(x)$  is the tangential displacement and  $u_2 = u_2(x)$  is the normal displacement. Here  $x \in [0, 2\pi]$  represents the angular coordinate on the cross-section of the torus. Moreover, we consider a torus having a unitary section radius and we set  $R > 1$  as the distance between the principal axis and the center of the circular cross-sections. We also need to define the scalar  $K$ , the matrix  $A$  and the operators  $\alpha_i, \beta_i$  as

$$K = \frac{E}{12(1 - \nu^2)}, \quad A_{ii} = 1, \quad A_{ij} = \nu, \quad (i \neq j) \tag{50}$$

for  $i, j = 1, 2$ ,

$$\alpha_1(\underline{v}) = \frac{1}{(a_3)^2} [(2a_0 a_1 + R a_0) v_1 - (a_1)^2 v_2 - a_0 a_3 v_2'], \tag{51}$$

$$\alpha_2(\underline{v}) = v_2'' - v_2 - 2v_1', \tag{52}$$

$$\beta_1(\underline{v}) = \frac{1}{(a_3)^2} (-a_2 v_1 + a_3 a_1 v_2), \quad \beta_2(\underline{v}) = v_1' + v_2, \tag{53}$$

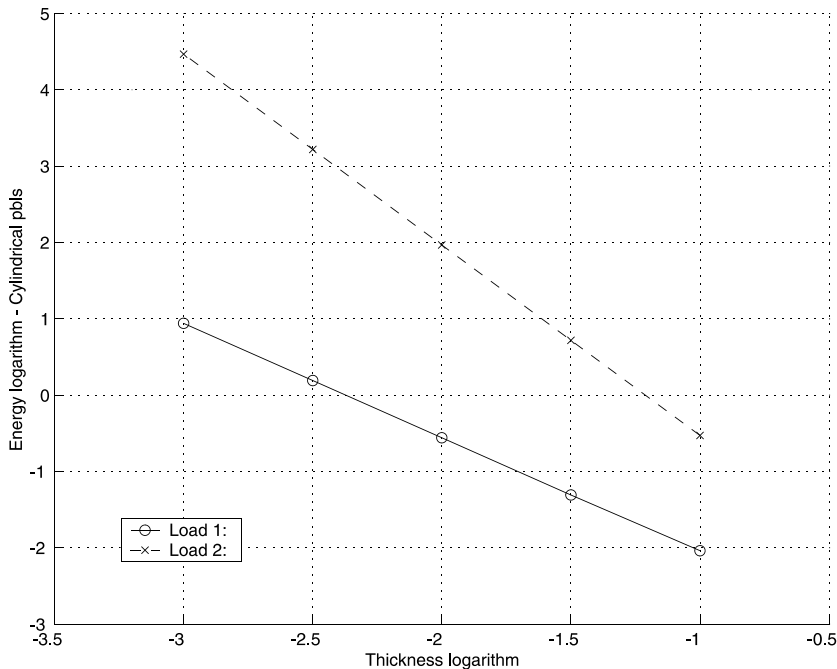


Fig. 1.  $\log E_h(\varepsilon)$  vs  $\log \varepsilon$ : cylindrical shell pbls.

where the periodic functions  $a_i(x)$  are given by

$$a_0 = \sin x, \quad a_1 = \cos x, \tag{54}$$

$$a_2 = \sin x(R + \cos x), \quad a_3 = R + \cos x. \tag{55}$$

The bilinear forms  $a^b(\cdot, \cdot)$  and  $a^m(\cdot, \cdot)$  takes the form

$$a^b(\underline{u}, \underline{v}) = K \int_0^{2\pi} \sum_{i,j=1}^2 \alpha_i(\underline{u}) A_{ij} \alpha_j(\underline{v}) a_3 \, dx, \tag{56}$$

$$a^m(\underline{u}, \underline{v}) = 12K \int_0^{2\pi} \sum_{i,j=1}^2 \beta_i(\underline{u}) A_{ij} \beta_j(\underline{v}) a_3 \, dx. \tag{57}$$

For this shell the space  $\mathcal{U}$  of admissible displacements is given by

$$\mathcal{U} = \left\{ \underline{v} \in H_{\sharp}^1(0, 2\pi) \times H_{\sharp}^2(0, 2\pi) : v_2 \left( \frac{3\pi}{2} \right) = 0 \right\},$$

where the additional constraint is to prevent rigid body motions, and the subscript  $\sharp$  means that periodic boundary conditions are imposed. It is easily seen that also in this case  $\mathcal{U} = V$ . Finally, the three different problems correspond to the following loads (in  $V$ ):

$$\langle f_1, \underline{v} \rangle = -Kv_2(\pi), \tag{58}$$

$$\langle f_2, \underline{v} \rangle = -Kv_2(0), \tag{59}$$

$$\langle f_3, \underline{v} \rangle = -Kv_2 \left( \frac{\pi}{2} \right). \tag{60}$$

In the toroidal problems the characterization of the completion  $W$  of  $V$  by means of the norm induced by the form  $a^m(\cdot, \cdot)$  seems to be much more difficult than in the cylindrical case. The principal difficulty stands in the complicated shape of  $a^m(\cdot, \cdot)$ . For example we proved that such norm cannot be broken into the sum of two norms acting separately on the two different displacement components, at least when the natural basis is used. Even though we did not succeed in a full characterization of  $W$ , we nonetheless were able to prove the following proposition (refer to [12]), which gives some insight about the structure of the space  $W$ .

**Proposition 9.** *There exist two positive real numbers  $C_1, C_2$  such that*

$$\|\underline{u}\|_W \leq C_1 (\|u'_1\|_{L^2} + \|u_2\|_{L^2}), \tag{61}$$

$$\|\underline{u}\|_W \geq C_2 (\|u'_1 \cos x\|_{L^2} + \|u_2 \cos x\|_{L^2} + \|u_1 \cos x\|_{L^2}), \tag{62}$$

for every  $\underline{u} = (u_1, u_2) \in V$ . Neither of the norms in the right-hand side of (61) and (62) is equivalent to  $\|\cdot\|_W$ .

Such a proposition can be used to provide a first (although not completely rigorous) study of the toroidal shell, arguing as follows. From (62) it appears that the problem with the norm in the right-hand side consists in its “weight”  $\cos x$ , which vanishes in  $\pi/2$  and  $3\pi/2$ . Thus, let  $\bar{\omega}$  be any subdomain defined excluding from  $[0, 2\pi]$  two arbitrary small neighbourhoods of the points  $\pi/2, 3\pi/2$ . Using Proposition 9 it is easy to obtain the norm equivalence

$$W|_{\bar{\omega}} \simeq H_{\sharp}^1(\bar{\omega}) \times L^2(\bar{\omega}), \tag{63}$$

where the subscript  $\sharp$  retains the meaning of periodic boundary conditions for 0 and  $2\pi$ . Considering the first two problems associated with the choice  $f_1$  and  $f_2$  (cf. (58) and (59)), we see that their application points are both “rather far” from the critical points  $\pi/2$  and  $3\pi/2$ . Therefore, due to (63) it seems to be reasonable to conjecture that substituting  $W$  with

$$H_{\sharp}^1(0, 2\pi) \times L^2(0, 2\pi) \tag{64}$$

should not change the problem orders. This non-rigorous argument leads to a problem order prevision equal to 3/2 for both loads  $f_1$  and  $f_2$ , which was exactly the result given by the numerical tests as depicted in Fig. 2 (for which we adopted the same method as in the cylindrical case). For the third problem (cf. (60)), where the load  $f_3$  acts on a critical point, we expect a different behaviour. We conjecture that the order of the problem should be  $\alpha_3 = 2$ , a value which is not far from the one obtained with the numerical tests (about 1.95). However, it would be interesting to exactly determine  $W$  and the corresponding interpolation spaces between  $V$  and  $W$ , in order to fully apply Theorem 4 in the toroidal case as well.

#### 5.4. The Scordelis-Lo roof

The Scordelis-Lo roof, essentially a cylindrical roof loaded by a constant vertical load, has achieved the status of a standard benchmark for shell numerical methods (cf. [26]). The variational formulation is as follows. We consider a cylindrical shell of thickness  $\varepsilon$  and unitary radius described by the region

$$\Omega = \{(x, \varphi, z) \mid -1 \leq x \leq 1, \quad -2\pi/9 \leq \varphi \leq 2\pi/9, \quad -\varepsilon/2 \leq z \leq \varepsilon/2\}. \tag{65}$$

Above,  $x$  is the axial coordinate,  $z$  the radial one and  $\varphi$  is the angular coordinate for which the vertical direction corresponds to  $\varphi = 0$ . We call  $\omega$  the midsurface of the shell. The unknowns are  $u = u(x, \varphi)$  (the axial displacement),  $v = v(x, \varphi)$  (the angular displacement) and  $w = w(x, \varphi)$  (the radial or normal displacement). Furthermore, the membrane strains are given by

$$\gamma_{11} = u_{,x}, \quad \gamma_{12} = \frac{1}{2}(u_{,\varphi} + v_{,x}), \quad \gamma_{22} = v_{,\varphi} + w. \tag{66}$$

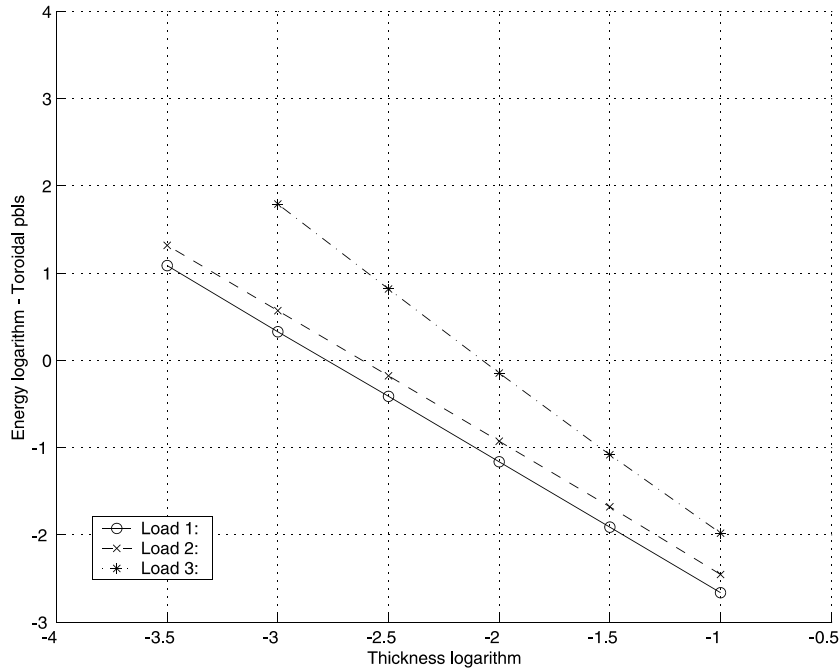


Fig. 2.  $\log E_h(\varepsilon)$  vs  $\log \varepsilon$ : toroidal shell pbls.

The bending strains are

$$\Upsilon_{11} = w_{,xx}, \quad \Upsilon_{12} = w_{,x\varphi} - v_{,x}, \quad \Upsilon_{22} = w_{,\varphi\varphi} - 2v_{,\varphi} - w. \tag{67}$$

Introducing the notation  $\underline{u} = (u, v, w)$ , the membrane and bending energy forms are given by

$$\begin{aligned} \varepsilon a^m(\underline{u}, \underline{u}) := & \frac{\varepsilon}{2} \int_{\omega} \left[ v(\gamma_{11}(\underline{u}) + \gamma_{22}(\underline{u}))^2 \right. \\ & \left. + (1 - \nu) \sum_{i,j=1}^2 \gamma_{ij}(\underline{u}) \right] dx, \end{aligned} \tag{68}$$

$$\begin{aligned} \varepsilon^3 a^b(\underline{u}, \underline{u}) := & \frac{\varepsilon^3}{24} \int_{\omega} \left[ v(\Upsilon_{11}(\underline{u}) + \Upsilon_{22}(\underline{u}))^2 \right. \\ & \left. + (1 - \nu) \sum_{i,j=1}^2 \Upsilon_{ij}(\underline{u}) \right] dx, \end{aligned}$$

where  $\nu$  is the Poisson’s ratio. We apply a constant vertical load, so that the external energy can be written as

$$\langle f, \underline{u} \rangle = f_0 \int_{\omega} (v \sin \varphi - w \cos \varphi) dx. \tag{69}$$

The admissible displacement space is given by

$$\mathcal{U} = \{H^1(\omega) \times H^1(\omega) \times H^1(\omega)\} \cap \mathcal{B}\mathcal{C}, \tag{70}$$

where  $\mathcal{B}\mathcal{C}$  stands for boundary conditions and the space is equipped with the usual norm. We investigate the roof

energy behaviour under the following three different sets of boundary conditions.

*Case 1:* We set  $v = w = 0$  on the curved boundaries  $\{x = \pm 1, -2\pi/9 \leq \varphi \leq 2\pi/9\}$ . This is the classical Scordelis-Lo problem.

*Case 2:* The roof is clamped along the whole boundary:  $u = v = w = 0$  on  $\{-1 \leq x \leq 1, \varphi = \pm 2\pi/9\} \cup \{x = \pm 1, -2\pi/9 \leq \varphi \leq 2\pi/9\}$ .

*Case 3:* The roof is clamped ( $\underline{u} = 0$ ) along its straight boundaries  $\{-1 \leq x \leq 1, \varphi = \pm 2\pi/9\}$ .

The problem was solved numerically using the quadrilateral finite element scheme presented in [27] available in the research-oriented code FEAP (see [26]). Due to the symmetry we model only one fourth of the roof, using a uniform  $128 \times 128$  mesh. We obtained the following results:

*Case 1:* For the classical Scordelis-Lo roof problem it is easily verified that for the load at hand we have  $f \in \mathcal{U}'_1$ . Moreover, following the proof in the appendix of [1], it is not hard to show that  $f \notin W'$ . Consequently, this shell problem falls into the intermediate category. So far, there are no theoretical arguments about the Scordelis-Lo roof problem order. However, the numerical tests displayed in Fig. 3, suggest a problem order of about  $7/4$ .

*Case 2:* Due to the imposed boundary conditions, we have that the space  $\mathcal{U}_1$  of inextensional displacements is trivial. Moreover, it can be shown that  $f \in W'$ . Therefore the shell is membrane dominated, and the problem order is 1. Our numerical results perfectly agree with the

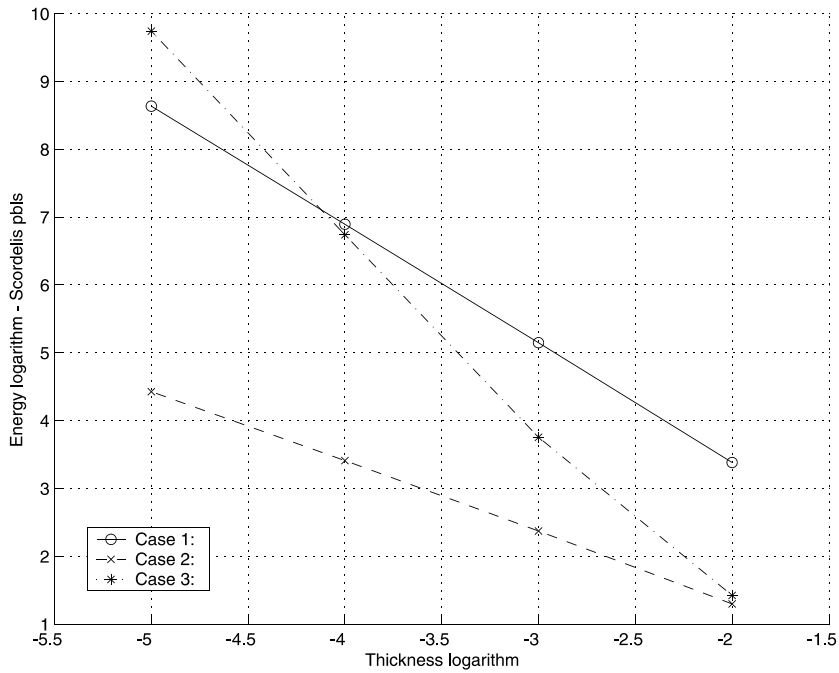


Fig. 3.  $\log E_h(\varepsilon)$  vs  $\log \varepsilon$ : Scordelis-Lo pbls.

above theoretical prediction, as shown by the slope of the graph in Fig. 3 corresponding to this case.

*Case 3:* With these boundary conditions, it can be seen that the space  $\mathcal{U}_1$  is non-trivial. Furthermore, an easy computation shows that  $f \in \mathcal{U}_1^0$ , i.e. there exist pure bending displacements  $v \in \mathcal{U}_1$  activated by the given load. Therefore the shell is bending dominated and the problem order is 3. Again, the accordance between the theoretical analysis and the numerical results can be appreciated in Fig. 3.

5.5. Local bending energy percentage

In what follows, we report some numerical results concerning the distribution of the bending energy percentage for the toroidal shell subjected to Dirac ring force  $f_3$  (cf. (60)). In each element  $I$  of the mesh we computed the local ratio

$$R_h(\varepsilon)|_I := \frac{\varepsilon^3 a^b(\underline{u}_h, \underline{u}_h)|_I}{E_h(\varepsilon)|_I} \tag{71}$$

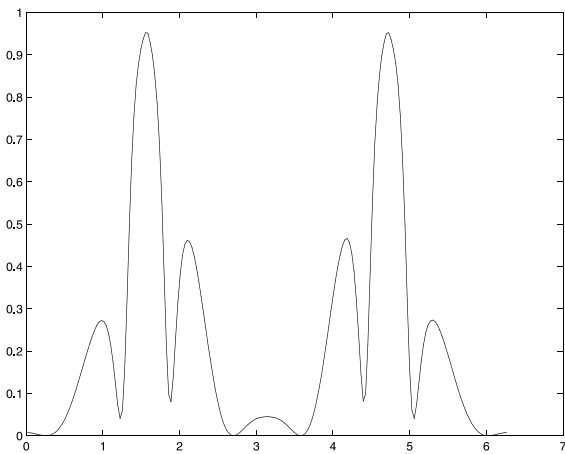


Fig. 4. Distribution of bending energy percentage,  $\varepsilon = 10^{-1}$ .

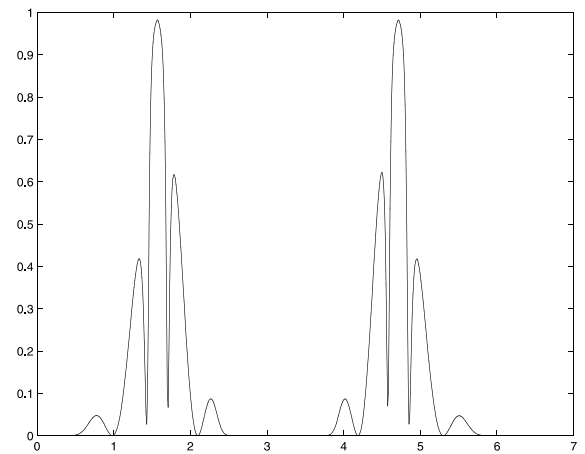


Fig. 5. Distribution of bending energy percentage,  $\varepsilon = 10^{-2}$ .

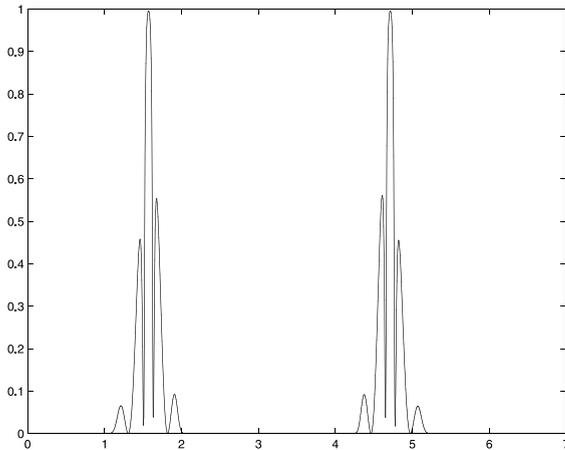


Fig. 6. Distribution of bending energy percentage,  $\varepsilon = 10^{-3}$ .

for different choices of the thickness  $\varepsilon$ . The distributions of the values for the above percentage are displayed in Figs. 4–6. Such graphs show not only a bending percentage concentration as the thickness decreases, but also highlight the presence of strong oscillations. The waves seem, as the thickness tends to zero, to grow in frequency and gather around the constraint ( $x = 3\pi/2$ ) and the load application point ( $x = \pi/2$ ). We remark that similar behaviours have been observed also for the other toroidal and cylindrical problems we have considered. Since we used a very fine mesh, we are sure that this oscillating behaviour is not an effect of numerical instabilities (for more details about this point, see [12]). The consequences of these results, especially in connection with the possibility to design a robust finite element scheme for intermediate shells, surely require much deeper investigations.

### Acknowledgements

The authors would like to thank Prof. K.J. Bathe, MIT for the very valuable comments on the first draft of the manuscript.

### References

- [1] Chapelle D, Bathe KJ. Fundamental considerations for the finite element analysis of shell structures. *Comput Struct* 1998;66(1):19–36.
- [2] Chapelle D, Bathe KJ. The mathematical shell model underlying general shell elements. *Int J Numer Methods Eng* 2000;48:289–313.
- [3] Chapelle D, Bathe KJ. *The finite element analysis of shells*. Berlin: Springer-Verlag; in press.
- [4] Ciarlet PG. *Introduction to linear shell theory*. Series in applied mathematics. Paris: Gauthier-Villars; 1998.
- [5] Gol'denveizer AL. *Theory of elastic thin shells*. Oxford: Pergamon Press; 1961.
- [6] Ciarlet PG. Mathematical modelling of linearly elastic shells. *Acta Numer* 2001;10:103–214.
- [7] Bathe KJ. *Finite element procedures*. Englewood Cliffs, NJ: Prentice-Hall; 1996.
- [8] Piila J, Leino Y, Ovaskainen O, Pitkäranta J. Shell deformation states and the finite element method: a benchmark study of cylindrical shells. *Comput Methods Appl Mech Eng* 1995;128:81–121.
- [9] Bathe KJ, Iosilevich A, Chapelle D. An evaluation of the MITC shell elements. *Comput Struct* 2000;75:1–30.
- [10] Chapelle D. Some new results and current challenges in the finite element analysis of shells. *Acta Numer* 2001;10: 215–50.
- [11] Baiocchi C, Lovadina C. A shell classification by interpolation. *Math Models Methods Appl Sci*, submitted for publication.
- [12] Beirão da Veiga L. Theoretical and numerical study of shell intermediate states on particular toroidal and cylindrical problems. *Ist Lomb Cad Sci Let Rend, (A)*, in press.
- [13] Beirão da Veiga L. Uniform error estimates for a class of intermediate cylindrical shell problems, in press.
- [14] Bergh J, Löfstrom J. *Interpolation spaces: an introduction*. Berlin: Springer-Verlag; 1976.
- [15] Lions JL, Peetre J. Sur une classe d'espaces d'interpolation. *Publ IHES* 1964;19:5–68.
- [16] Baiocchi C, Savaré G. Singular perturbation and interpolation. *Math Models Methods Appl Sci* 1994;4:557–70.
- [17] Lee PS, Bathe KJ. On the asymptotic behavior of shell structures and the evaluation in finite element solutions. *Comput Struct*, in press.
- [18] Blouza A, Le H. Existence and uniqueness for the linear Koiter model for shells with little regularity. *Quart Appl Math* 1999;57(2):317–37.
- [19] Bernadou M, Ciarlet PG. Sur l'ellipticité du modèle linéaire de W.T. Koiter. In: Glowinski R, Lions JL, editors. *Computing methods and engineering*. Berlin: Springer; 1976.
- [20] Sanchez-Palencia E. Statique et dynamique des coques minces. II. Cas de flexion pure inhibée—approximation membranaire. *CR Acad Sci Paris* 1989;309(I):531–7.
- [21] Blouza A, Brezzi F, Lovadina C. A new classification for shell problems. *Publicazioni IAN-CNR no. 1128*, 1999.
- [22] Blouza A, Brezzi F, Lovadina C. Sur la classification des coques linéairement élastiques. *CR Acad Sci Paris* 1999;328(I):831–6.
- [23] Chenais D, Paumier JC. On the locking phenomenon for a class of elliptic problems. *Numer Math* 1994;67:427–40.
- [24] Sanchez-Palencia E. Statique et dynamique des coques minces. I. Cas de flexion pure non inhibée. *CR Acad Sci Paris* 1989;309(I):411–7.
- [25] Lions JL, Sanchez-Palencia E. Problèmes sensitifs et coques élastiques minces. In: Cea J et al., editors. *Partial differential equations and functional analysis*. Basel: Birkhäuser; 1996.
- [26] Zienkiewicz OC, Taylor RL. *Finite element method*. 5th ed. Solid mechanics, vol. 2. Oxford: Butterworth-Heinemann; 2000.
- [27] Taylor RL. Finite element analysis of linear shell problems. In: *The mathematics of finite elements and applications VI, MAFELAP 1987, 1988*. p. 191–203.